AIAA JOURNAL
Vol. 38, No. 8, August 2000

Optimal Wing Planform Design for Aeroelastic Control

Changho Nam* and Aditi Chattopadhyay†
Arizona State University, Tempe, Arizona 85287-6106
and
Youdan Kim‡
Seoul National University, Seoul 151-742, Republic of Korea

An integrated aeroservoelastic design synthesis for flutter suppression and gust load reduction using multiple control surfaces is presented. For this multidisciplinary optimization procedure, structural design variables, control system, and aerodynamic design variables, such as wing planform, ply orientation of the composite layer, and control surface size and location, are considered simultaneously. The analysis for a composite wing with control surfaces is conducted by the finite element method. Unsteady aerodynamic forces calculated by the doublet lattice method are approximated as transfer functions of the Laplace variable by Roger's method. The output feedback control scheme is applied to design the active control system. Using a swept wing model, the performance of the control system is investigated. The geometry of wing planform and control surface size and location are determined by using the genetic algorithm. Design objectives are to minimize the control performance index and the root mean square of the gust responses for various airspeeds. Numerical results showed substantial improvements in performance index value as well as the root-mean-square values of the gust responses compared with the baseline wing model.

Introduction

WITH the development of lightweight, high-performance aircraft, it has become increasingly important to account for the aeroelastic responses, such as flutter and gust response. An active control system is necessary to suppress flutter or to alleviate the gust loads of a flexible wing. The study of aeroservoelastic tailoring to exploit the interaction of aerodynamics, elastic structures, and controls was reported by many authors.[1,2] During the past few decades, a number of analytical and experimental studies on aeroservoelastic control problems have been performed by utilizing a variety of synthesis techniques. The interactions of lightweight composite wing structures, steady and unsteady aerodynamics, and active control technology led to considerable multidisciplinary design challenges.[3] To overcome the complexity of the design problem and the associated high computational cost, procedures such as multilevel decomposition technique and analytical sensitivity analysis have been suggested.[4,5]

The goal of this study is to conduct an aeroservoelastic wing planform design by using the control surfaces to suppress flutter and to reduce the gust response of the wing. An optimization technique is used to find the best wing planform geometry and control surfaces geometry. The wing taper ratio, sweep angle, and control surfaces locations and sizes are included as design variables. The intent is to investigate the effects of the control surface locations on aeroelastic control. The output state feedback control law is used for aeroelastic control. The study compares the control performance index value as well as the gust response root-mean-square (rms) for the baseline and the optimized models.

Mathematical Aeroservoelastic Model

The equations of motion for aeroservoelastic analysis can be written as

$$[M_s]\{\ddot{q}\} + [C_s]\{\dot{q}\} + [K_s]\{q\} + [M_c]\{\ddot{\delta}_c\} = [Q_a]\{q\} + [Q_c]\{\delta_c\} + [Q_G](W_G/V) = q_d([A_a]\{q\} + [A_c]\{\delta_c\} + [A_G](W_G/V)) \tag{1}$$

where $\{q\}$ are the generalized modal coordinates and q_d is the dynamic pressure. The matrices $[Q_a]$, $[Q_c]$, and $[Q_G]$ are the generalized aerodynamic forces due to flexible modes, control surfaces deflection, and gust, respectively. A wing with control surfaces is modeled as a composite box beam (Fig. 1).

The structural analysis is conducted by using a finite element method.[6] After vibration analysis, a modal reduction is performed using the first six elastic modes. A doublet lattice method is used to compute the unsteady aerodynamic forces and the unsteady gust forces. The aerodynamic forces are approximated as the transfer functions of the Laplace variable by a least-square curve fit approximation in order to define the aeroservoelastic equations of motion in a linear time invariant state-space form. Roger's method[7] approximates the unsteady aerodynamic forces in the following form:

$$[A_{ap}] = [A_\xi \quad A_c \quad A_g] = [\bar{P}_0] + [\bar{P}_1]s' + [\bar{P}_2]s'^2 + \sum_{j=3}^{N} \frac{[\bar{P}_j]s'}{s' + \gamma_{j-2}} \tag{2}$$

where $\bar{P} = [P_\xi \quad P_c \quad P_g]$, $s' = ik = i\omega b/V = sb/V$, s is the Laplace variable, k is the reduced frequency, b is the semichord, and V is the airspeed. The subscripts ξ, c, and g indicate elastic, control surface, and gust modes, respectively, and γ_{j-2} are the aerodynamic poles, which are usually preselected in the range of reduced frequencies of interest. In this study, four terms of the aerodynamic poles are included for the rational functions approximation. The augmented aerodynamic state is defined as follows:

$$\{x_{ja}\} = \frac{s'}{s' + \gamma_{j-2}}[P_{j\xi} \quad P_{jc} \quad P_{jg}] \begin{Bmatrix} \xi \\ \delta_c \\ w_g \end{Bmatrix}, \qquad j = 3, 4, 5, 6 \tag{3}$$

It has to be noted that P_{2g} is set to be zero to avoid $\dot{w}_g$ term in the state equation. Therefore,

$$[A_g] = [P_{0g}] + [P_{1g}]s' + \sum_{j=3}^{N} \frac{[P_{jg}]s'}{s' + \gamma_{j-2}} \tag{4}$$

Received 5 October 1998; accepted for publication 14 January 2000.

*Visiting Faculty, Mechanical and Aerospace Engineering; Senior Engineering Specialist, ZONA Technology, Sottsdale, AZ 85251. Senior Member AIAA.

†Professor, Mechanical and Aerospace Engineering. Associate Fellow AIAA.

‡Associate Professor, Department of Aerospace Engineering. Senior Member AIAA.

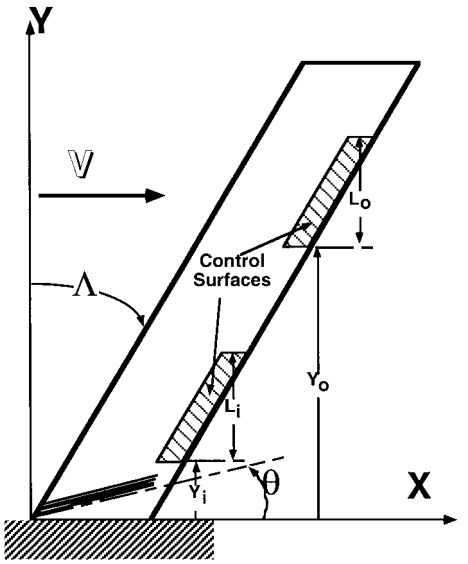

Fig. 1 Composite wing model with control surfaces.

Using the rational function approximation, the system equation of motion is written in the following form:

$$\{\dot{x}_s\} = [A_s]\{x_s\} + [B_s]\{u_s\} + [B_G]\{W_G\} \tag{5}$$

where

$$\{x_s\} = \lfloor \xi^T \quad \dot{\xi}^T \quad x_a^T \rfloor^T \tag{6a}$$

$$\{u_s\} = \lfloor \delta_{c1} \quad \dot{\delta}_{c1} \quad \ddot{\delta}_{c1} \quad \delta_{c2} \quad \dot{\delta}_{c2} \quad \ddot{\delta}_{c2} \rfloor^T \tag{6b}$$

$$\{w_G\} = \lfloor w_g, \dot{w}_g \rfloor^T \tag{6c}$$

In these equations, x_a denotes the aerodynamic states and δ_c is the control surface deflection. The control surfaces actuator transfer functions can be expressed in a state-space form as follows:

$$\{\dot{x}_c\} = [A_c]\{x_c\} + \{B_c\}\{\delta_{\text{aileron}}\}, \qquad \{u_s\} = [C_c]\{x_c\} \tag{7}$$

The actuator transfer function for each of the control surfaces is preassigned as follows:

$$\frac{\{\delta_c\}}{\{\delta_{\text{ailtron}}\}} = \frac{20}{s + 20} \frac{1.6 \times 10^5}{s^2 + 400s + 1.6 \times 10^5} \tag{8}$$

The gust state-space model is included for random gust response calculations. The vertical gust is modeled by a second-order Dryden model:

$$\frac{w_g}{w} = \sigma_{wg} \frac{\sqrt{3V/L}\left[s + \left(V/L\sqrt{3}\right)\right]}{[s + (V/L)]^2} \tag{9}$$

where σ_{wg} is the rms value of the gust velocity, L is the characteristic gust length, and V is the airspeed. When the low-pass filter is included, the state-space equation of the gust is expressed as follows:

$$\{\dot{x}_g\} = [A_g]\{x_g\} + \{B_g\}w, \qquad \{w_G\} = [C_g]\{x_g\} \tag{10}$$

By including the gust dynamics system and the actuator system for the control surface, the following state-space aeroservoelastic model is obtained:

$$\{\dot{x}\} = [A]\{x\} + [B]\{u\} + \{B_w\}w, \qquad \{y\} = [C]\{x\} \tag{11}$$

where $\{x\}^T = \lfloor x_s^T \quad x_c^T \quad x_g^T \rfloor$. The resulting state-space model is 45th order including 6 elastic modes, 24 aerodynamic states, 6 actuator states, and 3 gust states.

Controller Design

Pole Placement Technique

For a given design airspeed, a controller for active flutter suppression is designed. The performance index value (control effort) is used as a measure of control performance. The following output feedback control law is introduced:

$$\{u\} = -[K_G]\{y\} \tag{12}$$

where $[K_G]$ denotes output feedback gain and $\{y\}$ includes only structural information. The eigenvalue problem of the closed-loop system can be written as

$$([A] - [B][K_G][C])\{\phi^c\}_i = \lambda_i^c \{\phi^c\}_i \tag{13}$$

where $\{\phi^c\}_i$ is the eigenvector of the closed-loop system corresponding to the eigenvalue λ_i^c. The eigenvalues of the structural modes can be assigned to desired values by using a pole placement technique.

The problem can be stated as a nonlinear parameter optimization problem in which it is necessary to impose specified eigenspace equality constraints and the elements of output feedback gain matrix are the parameters to be determined. Defining $\{p\}$ as the parameter vector that consists of the elements of output feedback gain $[K_G]$, the nonlinear programming problem can be formulated as follows:

Determine output feedback gain parameter $\{p\}$ subject to

$$f_i(\{p\}) = \lambda_i^d - \lambda_i(\{p\}) = 0, \qquad i = 1, 2, \ldots, Ns \tag{14}$$

where $f_i(\{p\})$ is the equality constraint equation that is related to the closed-loop eigenvalue assignment, Ns is the number of structural modes, and λ_i^d denotes the desired eigenvalues of these modes.

This problem can be solved by using any gradient-based nonlinear programming algorithm. In this study, homotopic nonlinear programming with minimum norm correction algorithm is used.[8,9] To enhance convergence, the linear homotopy map is generated. The original eigenvalue assignment problem is replaced by the one-parameter α family as follows:

$$\begin{aligned} f_i(\{p\}) &= \alpha\lambda_i^d + (1 - \alpha)\lambda_i(\{p_{\text{start}}\}) - \lambda_i(\{p\}) \\ &= 0, \qquad 0 \le \alpha \le 1 \end{aligned} \tag{15}$$

where $\{p_{\text{start}}\}$ is the initial starting value of the parameter vector. Sweeping α using a suitably small increment generates a sequence of neighboring problems. These sequences of problems are solved using the neighboring converged solutions to generate starting iterative for each subsequent problem. The desired solution is reached once solution for $\alpha = 1$ is obtained.

The local design corrections for each α are performed by linearizing the neighboring problem (nonlinear constraint equations) about the local solution and computing the minimum norm differential correction that satisfies the linearized constraint equation.[10] This algorithm is a generalized Newton procedure for solving a system of underdetermined nonlinear equations. On each iteration, the norm of the correction vector is minimized while the following linearized constraint equation is satisfied:

$$\left\{\frac{\partial f}{\partial p}\right\}\Bigg|_{\{p\}} \{\Delta p\} = -f(\{p\}) \tag{16}$$

where $f\{p\}^T = \{f_1\{p\}, f_1\{p\}, \ldots, f_{2Ns}\{p\}\}$ is a constraint vector. The solution of this equation can be obtained by the pseudoinverse of matrix $\{\partial f/\partial p\}|_{\{p\}}$, utilizing singular value decomposition.[11] The eigenvalue sensitivities required in this equation for iterative direction search can be evaluated by using the following analytical formulation[12]:

$$\frac{\partial \lambda_i^c}{\partial p_1} = \{\varphi^c\}_i^T \left(\frac{\partial([A] - [B][K_G][C])}{\partial p_1}\right)\{\phi^c\}_i \tag{17}$$

where $\{\varphi^c\}_i$ and $\{\phi^c\}_i$ are normalized right and left eigenvectors of the closed-loop system corresponding to the eigenvalue λ_i^c, respectively. Figure 2 shows the flowchart of this algorithm.

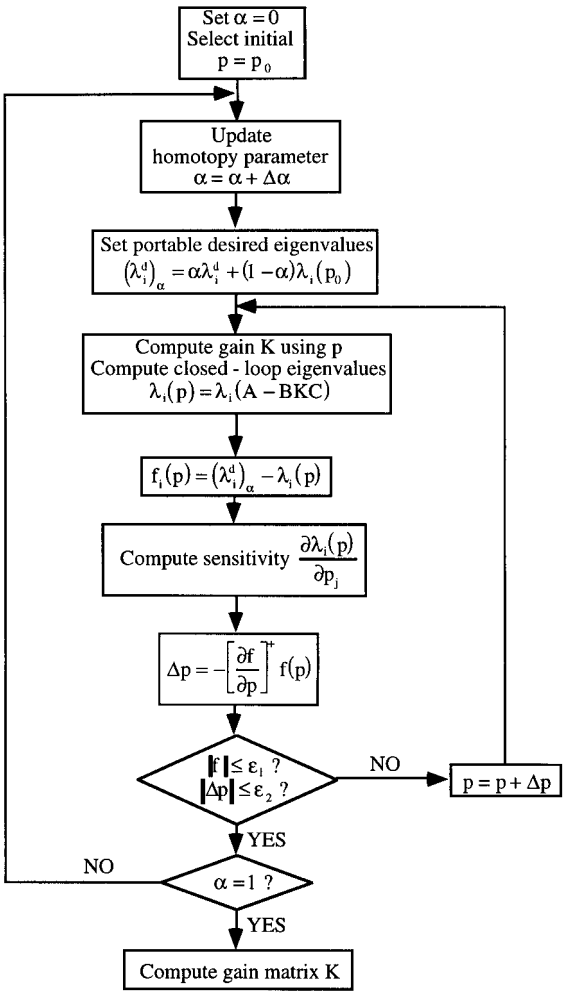

Fig. 2 Flowchart for control system design scheme.

Control Objective Function

A quadratic-type energy function is selected to represent the control objective function[13]:

$$J = \int_0^\infty \{\{y\}^T[Q]\{y\} + \{u\}^T[R]\{u\}\}\,dt \tag{18}$$

where the positive definite weight matrices $[Q]$ and $[R]$ should be related to make the integrands correspond to physical energy measures. Note that the first term in J is related to the error energy of the structural modes and the second term is related to the control energy. This objective function is obtained as follows[14]:

$$J = \text{tr}([P][X_0]) \tag{19}$$

where $[X_0]$ is an initial autocorrelation of the state and $[P]$ is the solution of the following Lyapunov equation:

$$[P][A_c] + [A_c]^T[P] + [C]^T\left([Q] + [K_G]^T[R][K_G]\right)[C] = 0 \tag{20}$$

where

$$[A_c] = [A] - [B][K_G][C] \tag{21}$$

The solution of the Lyapunov equation can be obtained by solving eigenvalue problem of the closed-loop system matrix $[A_c]$. However, it is unstable when the eigensystem is ill-conditioned. Because the aeroservoelastic system dealt with in this study is ill-conditioned, a Lyapunov solver, utilizing Schur decomposition,[15] is used. This algorithm transforms the closed-loop system matrix $[A_c]$ to the Schur form by orthogonal similarity transformation, computes the solution of the resulting triangular system, and transforms this solution back.

Another purpose of the control system is to prevent performance degradation due to external disturbances such as gust. For the gust load alleviation system, the rms values of gust response for the different modes are used as objective functions for performance comparison. The state covariance matrix $[X]$ of the closed-loop system is the solution of a Lyapunov equation in the form[16]

$$[A_c][X] + [X][A_c]^T + \{B_w\}[Q_w]\{B_w\}^T = 0 \tag{22}$$

where $[Q_w]$ is the intensity matrix of the white noise. The square of the rms of the system outputs (the modes of the system) is computed as follows:

$$\sigma_i^2 = [[C][X][C]^T]_{ii}, \qquad i = 1, 2, \ldots, Ns \tag{23}$$

Optimization Formulation

The formulation of this optimization problem may be stated as follows:

Find $\boldsymbol{X}$ to minimize $F(\boldsymbol{X})$ subject to

$$g_j(\boldsymbol{X}) \le 0, \qquad j = 1, 2, \ldots, m, \qquad \boldsymbol{X}_l \le \boldsymbol{X} \le \boldsymbol{X}_u$$

where $F(\boldsymbol{X})$ is the objective function, $\boldsymbol{X}$ is the design variables vector, the subscripts l and u represent lower and upper limits on design variables, respectively, and g_j is the inequality constraint. The objective function is defined as a linear summation of 25 index values, which are the performance index of the control system at the design airspeed, rms values of the first three displacements, and rate modes due to gust at the given airspeeds of 500, 1000, 1500, and 2000 ft/s. A total of eight design variables are used in this study. These are ply orientation of the composite layer θ, wing sweep angle Λ, taper ratio λ, aspect ratio AR, and spanwise location Y_i and size L_i of the control surfaces, as shown in Fig. 1. A total of 102 constraints are imposed: 10 constraints on the open-loop natural frequencies, 45 constraints on the stability of the open loop system at 1500 ft/s, 45 constraints on the stability of the closed loop system at 2000 ft/s, and 2 constraints on the inboard/outboard control surfaces to avoid overlapping.

Side constraints are also imposed on the design variables to remain within a specified boundary. These are as follows:

$$15 \le \Lambda \le 30, \qquad 0.5 \le \lambda \le 0.9, \qquad 2.0 \le AR \le 4.0$$

$$5\% \le Y_i \le 25\% \text{ of the span}$$

$$50\% \le Y_o \le 70\% \text{ of the span}$$

$$20\% \le L_i \le 25\% \text{ of the span}$$

$$20\% \le L_o \le 30\% \text{ of the span}$$

The genetic algorithm (GA) is used to solve this optimization problem.[17] Gradient-based optimization techniques have been applied successfully to many optimization problems. However, these methods tend to get trapped within local extrema. GAs have recently been applied to various structural problems and have demonstrated the potential of overcoming many of the problems associated with gradient-based methods. An exterior penalty function formulation can be adopted to transform a constrained optimization problem into an unconstrained optimization problem. In mathematical terms, the problem formulation becomes

$$\phi(\boldsymbol{X}) = \sum_{i=1}^{25} \frac{F_i(\boldsymbol{X})}{F_i(\boldsymbol{X}_0)} + R\sum_{j=1}^{m}\{\max[0, g_j(\boldsymbol{X})]\}^2 \tag{24}$$

where $\boldsymbol{X}_0$ is the initial values of the design variables and R is the penalty parameter. To maximize a fitness function in GA, the pseudo objective function is transformed as follows:

$$\Phi(\boldsymbol{X}) = \phi_{\max} - \phi(\boldsymbol{X}) \tag{25}$$

where $\phi_{\max}$ is chosen to be greater than the largest value of pseudo-objective function.

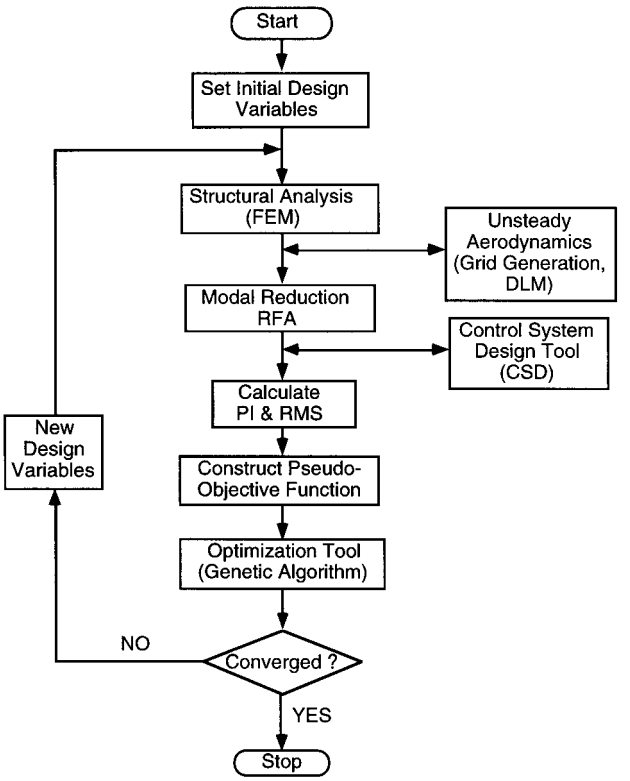

Fig. 3 Flowchart for the integrated structures/aerodynamics/control design process.

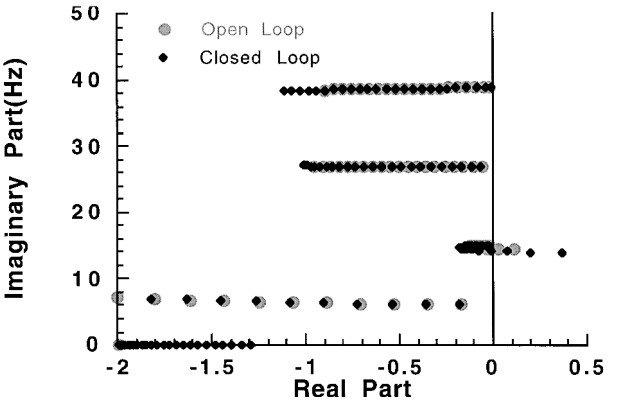

Fig. 4 Open-loop and closed-loop root loci of the baseline wing planform.

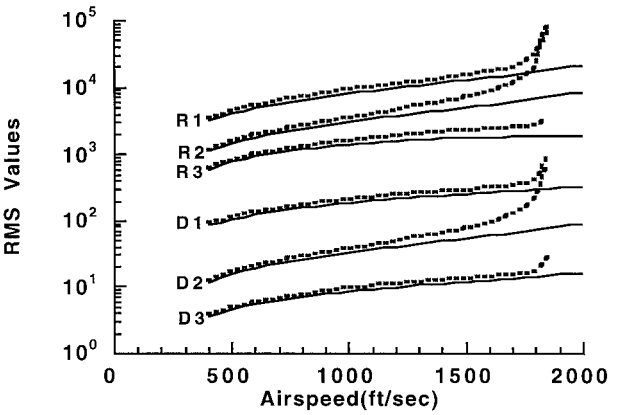

Fig. 5 RMS values of the displacement (Di) and rate (Ri) modes due to a gust for the baseline model: - - - -, open-loop system; and ——, closed-loop system.

The GA is based on the principles of natural genetics and natural selection. The design variables are represented as strings on binary variables that correspond to the chromosomes in natural genetics. The objective function value corresponding to design variables plays the role of fitness in natural genetics. A GA approach requires a population of chromosomes representing a combination of features from the set of features and a cost function (fitness function). The algorithm creates an initial population of size, which is created from a random selection of the parameters. Each parameter set represents the individual's chromosomes. Each of the individuals is assigned a fitness based on how well each individual's chromosomes allow it to perform in its environment. There are then three operations that occur in GAs to create the next generation: reproduction, crossover, and mutation. The process of mating and child creation is continued until an entirely new population of size is generated, with the hope that strong parents will create a fitter generation of children. Successive generations are created until very fit individuals are obtained. The flowchart of this optimization process is shown in Fig. 3.

Numerical Examples and Results

A composite wing model with inboard/outboard control surfaces is used as a base model for aeroelastic control system design. The baseline model has 25 deg of sweep angle, aspect ratio of 2.48, and taper ratio of 1. The wing area is set to be 1800 in.^{2} and is held fixed during the optimization process. The wing skin is composed of 14 symmetric composite layers, which are $[-90/+45/-45/\theta/+45/-45/-90]_s$. Each layer has uniform thickness, 0.008, 0.01, 0.01, 0.104, 0.01, 0.01, and 0.008 in. The inboard control surface is located at 20% of span. The spanwise size of the control surface is 25% of span (i.e., $Y_i = 20\%$, $L_i = 25\%$ of the span). The outboard control surface is located at 60% of span. The spanwise size of the control surface is 30% of span (i.e., $Y_o = 60\%$, $L_o = 30\%$ of the span). The chordwise size of each control surface is set to be 25% of chord.

For the baseline wing model with $\theta = 40$ deg, open-loop flutter analysis is conducted. Flutter occurs at 1850 ft/s (fps) and is due to the second mode. Figure 4 shows the control system design results, the root loci for the open loop and the closed loop when the control system is designed with a design velocity of 2000 fps. The closed-loop system flutters at 2250 fps. The second mode is shifted to the left to make the system be more stable. Figure 5 shows the rms plots of the displacement and velocity states due to a gust over a range of airspeed for closed-loop system. For comparison, the rms values of the open-loop system are also plotted as dashed lines. It can be seen that flutter does not occur over the entire airspeed range for the closed-loop system. As the airspeed is increased, the closed-loop rms values of the modes, especially the second mode, are decreased compared to the open-loop case.

Using this baseline model, the optimization technique is applied for both flutter suppression and gust load reductions. For this optimal design problem, the following parameters are used in GA: multiplication factor $=2$, mutation probability $=0.0333$, crossover probability $=0.6$, population size $=100$, and string length of each variable $=10$. Figure 6 shows the iteration history of the optimal design. The optimized performance index value J is 1.595×10^6, which is only 46% of the initial value, 3.461×10^6. The optimized geometry of the wing planform is shown in Fig. 7. The optimal ply angle is also shown. The optimal ply orientation is -65 deg. The optimal sweep angle, aspect ratio, and taper ratio are, respectively, 23 deg, 2.76, and 0.70. The location and spanwise size of the inboard and outboard control surfaces are $Y_i = 16.7\%$, $L_i = 22.2\%$, $Y_o = 58.8\%$, $L_o = 24.8\%$ of span.

Figure 8 plots the changes in the eigenvalues of the open, and the closed-loop systems for both the initial and the optimized configurations, respectively. It can be seen that the second mode of the closed loop for the optimized model becomes more stable than the initial case. Table 1 lists the rms values of the elastic modes due to a gust for the baseline and optimized models.

As shown in Table 1, all of the rms values for the optimized model are reduced. Especially, the rms values of second mode, which is unstable in the open-loop system, are reduced. This is due to the fact that a larger weight is imposed on the second mode when the flutter suppression system is designed.

Table 1 RMS values due to a gust for the baseline and optimized models at the design airspeed

Mode	Baseline model	RMS value optimized model
Displacement		
1	339.86	213.66(62%)
2	95.34	9.22(10%)
3	16.46	5.08(31%)
Rate		
1	21,903.97	10,653.54(49%)
2	8,536.39	538.96(6%)
3	1,818.07	702.77(39%)

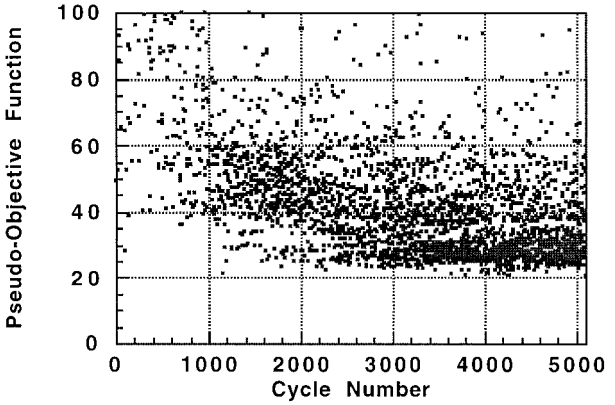

Fig. 6 Evaluation histories of the pseudo-objective function in the GA.

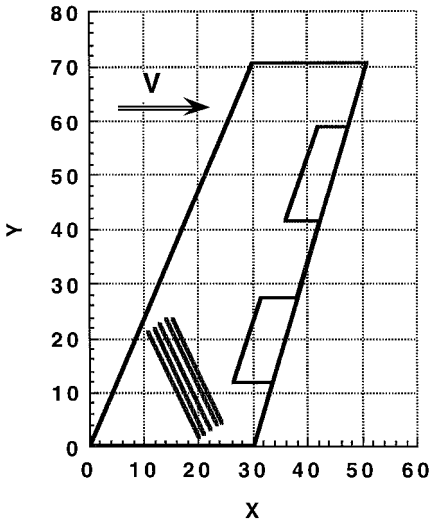

Fig. 7 Optimized geometry of the wing with control surfaces.

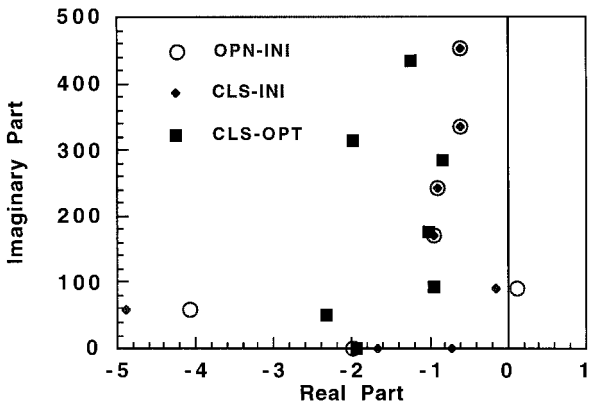

Fig. 8 Eigenvalue changes due to the flutter suppression system for the optimized and baseline wing models at design airspeed.

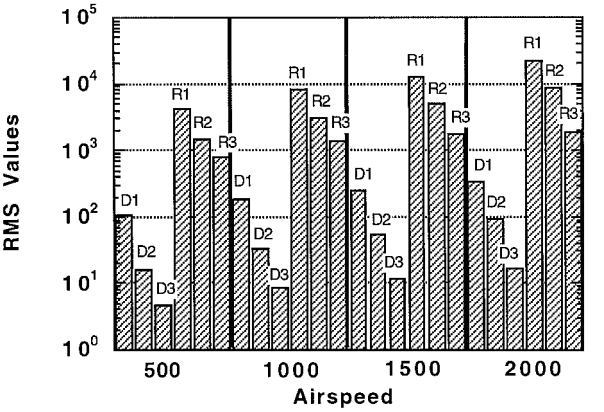

Fig. 9 RMS values of the modes due to disturbances for the base model.

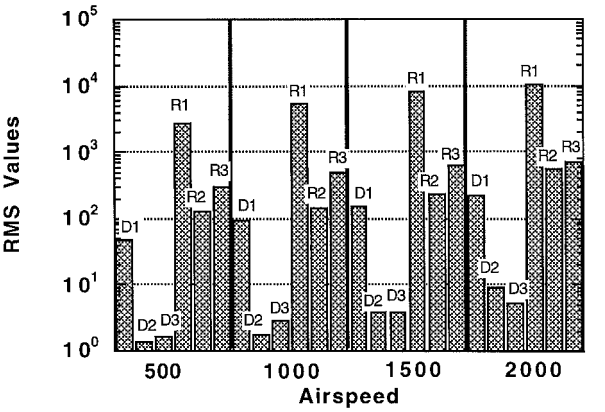

Fig. 10 RMS values of the modes due to disturbances for the optimized wing model.

Figures 9 and 10 plot the rms values of the first three displacement and rate modes of the closed-loop system due to a gust for the baseline and the optimized models, respectively. It can be seen that optimized wing geometry yields better control performance for both gust load reduction and flutter suppression. It also must be noted that the rms values of the second mode are significantly reduced compared to the baseline model because larger weight is imposed on the second mode.

Summary

The main purpose of this study is to conduct an integrated simultaneous aeroservoelastic design of a composite wing, incorporating control design parameters as well as aerodynamic parameters. The inboard and outboard control surfaces are used in suppressing flutter and in reducing the gust load of the wing. For a control design, the output state feedback control law is used for this study. The rms value of the gust response for the flexible modes and the control performance index are used as a metric to compare the control performance. Optimization technique is applied to find the best geometry of the wing planform with control surfaces for flutter suppression. The results show that the performance index is decreased about 54% compared to the baseline model. RMS values of the gust response due to a gust are also decreased. Future studies will take into account the static aeroelastic criteria, such as lift effectiveness, roll effectiveness, and induced drag as a part of the objective functions.

References

[1]Livne, E., "Integrated Aeroservoelastic Optimization: Status and Direction," *Journal of Aircraft*, Vol. 36, No. 1, 1998, pp. 122–145.

[2]Weisshaar, T. A., "Aeroservoelastic Control Concepts With Active Materials," 1994 International Mechanical Engineering Congress and Exposition, Nov. 1994.

[3]Chattopadhyay, A., Jury, R., IV, and Rajadas, J., "An Enhanced Multiobjective Formulation Technique for Multidisciplinary Design Optimization," AIAA Paper 97-0104, Jan. 1997.

[4]Livne, E., and Li, W.-L., "Aeroservoelastic Aspects of Wing/Control Surface Planform Shape Optimization," *AIAA Journal*, Vol. 33, No. 2, 1995, pp. 302–311.

[5]Li, W., and Livne, E., "Analytic Sensitivities and Approximations in Supersonic and Subsonic Wing/Control Surface Unsteady Aerodynamics," *Journal of Aircraft*, Vol. 34, No. 3, 1997, pp. 370–379.

[6]Layton, J. B., and Nam, C., "Multiobjective Reduced Order Control Design for Gust Alleviation Using and Covariance Control," AIAA Paper 97-1183, April 1997.

[7]Tiffany, S. H., and Adams, W. M., "Nonlinear Programming Extensions to Rational Function Approximation Methods for Unsteady Aerodynamic Forces," NASA TP-2776, 1998.

[8]Junkins, J. L., and Kim, Y., *Introduction to Dynamics and Control of Flexible Structures*, AIAA, Washington, DC, 1993, pp. 375–387.

[9]Dunyak, J. P., Junkins, J. L., and Watson, L. T., "Robust Nonlinear Least Square Estimation Using the Chow–Yorke Homotopy Method," *Journal of Guidance, Control, and Dynamics*, Vol. 7, No. 6, 1984, pp. 752–755.

[10]Junkins, J. L., "Equivalence of the Minimum Norm and Gradient Projection Constrained Optimization Techniques," *AIAA Journal*, Vol. 10, No. 7, 1972, pp. 927–929.

[11]Stewart, G. W., *Introduction to Matrix Computations*, Academic, New York, 1973, pp. 283–291.

[12]Lim, K. B., Junkins, J. L., and Wang, B. P., "Re-Examination of Eigenvector Derivatives," *Journal of Guidance, Control, and Dynamics*, Vol. 10, No. 6, 1987, pp. 581–587.

[13]Rew, D. W., Junkins, J. L., and Juang, J. N., "Robust Eigenstructure Assignment by a Projection Method: Applications Using Multiple Optimization Criteria," *Journal of Guidance, Control, and Dynamics*, Vol. 12, No. 3, 1989, pp. 396–403.

[14]Lewis, F. L., *Applied Optimal Control and Estimation*, Prentice–Hall, Englewood Cliffs, NJ, 1992, pp. 191–203.

[15]Bartels, R. H., and Stewart, G. W., "Solutions of Matrix Equation AX + XB = C," *Communications of ACM*, Vol. 15, No. 9, 1972, pp. 820–826.

[16]Livne, E., Schmit, L. A., and Friedmann, P. P., "Towards Integrated Multidisciplinary Synthesis of Actively Controlled Fiber Composite Wings," *Journal of Aircraft*, Vol. 27, No. 12, 1990, pp. 979–992.

[17]Goldberg, D. E., *Genetic Algorithms in Search, Optimization, and Machine Learning*, Addison–Wesley, Reading, MA, 1989, Chap. 4.

A. D. Belegundu
Associate Editor